DIELECTRIC BREAKDOWN IN MOS STRUCTURES OF Al_2O_3 ON Si DEPOSITED BY GAIVB TECHNIQUE

GAIVB 法에 의해 形成된 Al_2O_3/Si MOS 構造에서의 降伏現象에 관한 考察

成 萬 永*·金 天 燮*
(Man-Young Sung · Chun-Sub Kim)

요 약

本 論文에서는 Al_2O_3薄膜을 GAIVB(Gas Assisted and Ionized Vapour Beam)法에 의해 低溫에서 300Å-1400Å의 두께로 成長하여 그 條件을 提示하였다.

아울러 Al-Al_2O_3-Si의 MOS 構造를 製作하여 Breakdown 現象을 考察하고 그 結果를 分析 提示하므로써 GAIVB 法에 의해 低溫으로 形成된 Al_2O_3膜의 活用 可能性을 報告하였다.

한편, 本 硏究에서 製作한 Al_2O_3 薄膜의 抵抗率은 膜의 두께 100Å-1000Å인 試料素子에서 10^8 ohm-cm와 10^{13} ohm-cm로 測定되었고 比誘電率은 8.5-10.5, 絶緣破壞强度는 6~7 MV/cm (+바이어스)와 11~12MV/cm(-바이어스)이었다.

ABSTRACT

Aluminum oxide(Al_2O_3) offers some unique advantages over the conventional silicon dioxide(SiO_2) gate insulator: greater resistance to ionic motion, better radiation hardness, possibility of obtaining low threshold voltage MOS FETs, and possibility of use as in nonvolatile memory devices.

We have undertaken a study of the dielectric breakdown of Al_2O_3 on Si deposited by GAIVB Technique. In our experiments, we have varied the Al_2O_3 thickness from 300Å to 1400Å. The resistivity of Al_2O_3 films varies from 10^8ohm-cm for films less than 100Å to 10^{13}ohm-cm for films on the order of 1000Å.

The relative dielectric constant was 8.5-10.5 and the electric breakdown field was the 6-7 MV/cm (+bias) and the 11-12 MV/cm(-bias).

The average fields required to produce breakdown in 10^3 sec were approximately 4.5 MV/cm for

* 고려대학교 전기공학과

positive bias on either Al or Au field plates, 5.0 MV/cm for negative bias on Al and 6.5 MV/cm for negative bias on Au.

1. INTRODUCTION

The use of silicon dioxide (SiO_2) as an insulator has become so widespread in the microelectronics industry that it would seem almost unchangeable. Nevertheless, SiO_2 does not satisfy all criteria for an ideal technological insulator.

Therefore there have been investigations underway for some years by numerous workers searching for possible alternative insulators. [1-6] Among those which have been seriously studied are phosphosilicate glass(PSG), silicon nitride (Si_3N_4), and aluminum oxide(Al_2O_3). PSG was introduced to provide a better barrier to sodium ion penetration, for sodium can cause serious threshold instability problems in MOS FETs. Si_3N_4 was also studied with this role in mind, but it has proven useful as an etching and oxidation mask and as an insulator in nonvolatile memory devices as well. Aluminum oxide has some unique advantage over SiO_2 which makes it promising; greater resistance to ionic motion,[7-9] greater radiation hardness,[7] the possibility of obtaining low threshold voltage MOS FETs, and the possibility of use in nonvolatile memory devices. Balk[2] has proposed a set of criteria to be employed in the selection of insulators either instead of, or in conjunction with SiO_2; 1) high dielectric constant, 2) high breakdown strength () 1MV/cm), 3) an effective barrier against contaminants such as alkali ions and moisture, 4) etchable in liquid etchants at or near room temperature, 5) stable electrical properties when used as gate insulator in FET, 6) controllable electrical properties when used as nonvolatile memory elements.

Many of these requirements are fulfilled very well by Al_2O_3. Al_2O_3 is believed to be more resistant to ionic penetration than SiO_2. Insulating films on Ⅲ-V compounds must be deposited at lower temperature than 400℃ owing to the volatility of V group elements.

This is the reason that the formation of insulators by a high temperature process is not applicable. Therefore low temperature and no damage deposition process of insulating films are strongly required.

Low temperature deposition of crystalline insulating films on various kinds of semiconductor substrates are also of great interest in formation of MIS structures which can be applied to fabricate three dimensional integrated circuits. So we have Al_2O_3 films deposited by Gas Assisted and Ionized Vapour Beam Technology(GAIVB) at low temperature.[10-11] In this paper, details of the film deposition system and fundamental characteristics of the Al-Al_2O_3-Si structures were described and the dielectric breakdown of Al_2O_3 was studied.

2. FILM PREPARATION AND DEVICE FABRICATION

2-1. Al_2O_3/Si Structure Preparation

In our experiments, both n and p type silicon wafers of 4-6 ohm-cm resistivity were used.

The substrates were first cleaned with ammonia hydrogen peroxide-ammonia HCI. This was followed by a dry 1100℃ thermal oxidation in 3% HCl for 40 min. resulting in a 1000Å layer of SiO_2.

This SiO_2 layer was removed by etching in a 50% HF solution, rinsed in a cascade rinse for 10 min. then spun dry. Films were deposited at different conditions (ionization currents, acceleration voltage, and substrate temperature) and films were also deposited on Si (111) for MOS structures.

This technique is based on the formation of aluminum oxide when molten Al is evaporated in an oxygen atmosphere. Details of the GAIVB system are described in Fig. 1.

Deposition chamber was evacuated by diffusion pump with cooled trap until 1.0x10^{-7} Torr. and Al evapolant (99.999%) was heated to 1200℃-1500℃ in the BN or Quartz crucible with nozzle of 0.5-2mm in diameter and 1-3mm in length. Typical deposition conditions are listed in table 1.

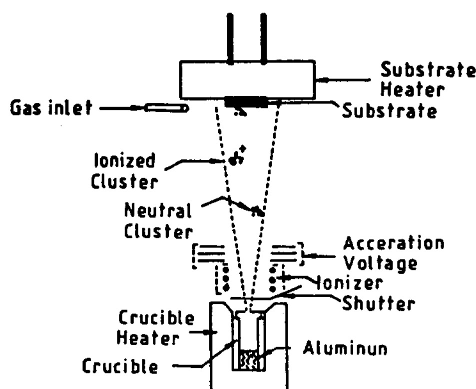

Fig. 1. Schematic Diagram of the Gas Assisted and Ionized Vapour Beam Epitaxy System.

Table. 1. Deposition conditions for Gas Assisted and Ionized Vapour Beam Technique.

Vacuum Pressure with O_2 Gas	1×10^{-4}Torr
Substrate Temperature	150−650℃
Acceleration Voltage	0−5kV
Ionizer Current	0−1.5 A
Nozzle Size	0.4−2.5 mm
Nozzle Length	(1−40)×Nozzle Size
Crucible Temperature	1200−1500℃

Oxygen is then allowed into the vacuum chamber with the aid of a needle valve control near the substrate holder. When the vacuum pressure reaches 1.5×10^{-4} Torr. The needle valve control is set such that equilibrium is reached between the incoming oxygen and the outgoing gases. During the evaporation Al and oxygen molecules collide increasing the aluminum oxide content of the evaporating gases. The efficiency of this collision process is determined by the capture cross sections of the particles involved and the partial pressure of the oxygen gas.

It is therefore very important to allow the oxygen to flow through the system prior to evaporation so that the percentage of oxygen gas in the bell jar or near the substrate reaches a saturation value. As the Al_2O_3 is evaporating, a shutter protecting the substrates from preparatory evaporations is opened. The shutter is then closed when the desired thickness of Al_2O_3 has been deposited on the substrate. After the oxide formation the substrate is placed in an oven at 150℃ for the post baking of a few min. This step is necessary to complete the oxide formation of Al molecules which did not interact with oxygen

molecules during the evaporation.

In our experiments, the Al_2O_3 thicknesses were about 300Å-1400Å. The oxide thicknesses were determined ellipsometrically (DHA-OL Ellipsometer) and varied by about 2% over the wafer for 450Å oxides and by as much as 5% over the wafer for the 900Å oxides. The samples had a heat treatment of 1000℃ for 30 minutes for annealing. As soon as possible, after the heat treatment, Al metallurgy is applied in the form of dots, in diameter, by evaporation followed by a post metallization annealing treatment of 400℃ for 30 minutes in N_2. All samples received a back contact of aluminum. The front contact was metallized with dot of aluminum. The samples used in our experiments had contact of thickness 1000Å with 0.080 cm diameter circular geometries, and area $2\times10^{-2}cm^2$ (square geometries).

The index of refraction was determined to vary from 1.68 to 1.73 over the entire set of wafers by Abeles Measurement System.

The relative dielectric constant was calculated by measuring the diameter of the dot under the optical microscope. The relation

$$C=\frac{\varepsilon_r\varepsilon_o A}{L}=\frac{\varepsilon_r\varepsilon_o}{L}\left(\frac{\pi}{4}d^2\right)$$

was then used to find the relative dielectric constant ε_r where ε_o=permittivity of vacuum=8.85×10^{-14}F/cm, L=oxide thickness, and d=diameter of metal dot on the Al_2O_3. The data taken over a number of capacitors on the same and on different wafers, gave a value of ε_r ranging from 8.5 to 10.5. The resistivity of Al_2O_3 films varies from 10^8 ohm-cm for films less then 100Å to 10^{13} ohm-cm for films on the order of 1000Å. Low temperature Al_2O_3 formation is performed by GAIVB technique. In our experiments, optimum conditions were 1 kV(acceleration voltage), 800 mA(Ionizer current) and 400 ℃ (substrate temperature).[10] Therefore electrical characteristics of Al_2O_3 films deposited at these conditions was measured and analyzed.

2-2. Measurement Techniques

The trapping of charge in the oxide is most readily observable in the time evolution of the C-V curves. The experimental procedure for obtaining these curves was as follows. The initial C-V curve was recorded by sweeping the sample from accumulation to inversion and back to accumulation. Then, the high field bias was applied for a given time. The C-V curve was then recorded, again sweeping from accumulation to inversion and back.

And also the electron current is induced in the Al_2O_3 using avalanche injection from the Si. A feedback circuit is used between the output of the electrometer and the 500 kHz square wave generator to control the amplitude of the square waves and keep the current in the Al_2O_3 constant at a value that is present as desired.

At trapping occurs, the square wave amplitude is automatically increased to compensate for the effect of the trapped charge. The square waves are interrupted periodically to measure automatically the flat band voltage as a means for monitoring the trapped charge build up in Al_2O_3. In the course of a typical run 400-600 measurements are made. These data are fed into a computer and results are analyzed to provide in-

formation concerning the trap cross sections and the traps densities. The computer program can resolve two different traps if their cross sections are separated by at least a factor of 2. The analysis of the results follows the same procedure followed by Di Maria.[4] The Al_2O_3 current used depends on the cross sections of interest and in this particular experiment the range was 9×10^{-11} to 10^{-9} A. The largest current is used for the small cross section traps. The change in the flat band voltage is given by Eq. (1), where Co is the Al_2O_3 capacity Do is the Al_2O_3 thickness, Qt is the trapped charge and $\bar{x}$ is the centroid of the trapped charge as measured with respect to the Al_2-Al_2O_3 interface.

$$\Delta V_{FB} = \frac{Qt\ \bar{x}}{Co\ Do} \quad (1)$$

The flat band voltage measurement does not enable us to determine Qt and $\bar{x}$ independently as a result we refer to an effective charge given by

$$Q_{effect} = \frac{Qt\ \bar{x}}{Do} \quad (2)$$

We obtain the cross sections and the effective trap densities by fitting exponentials to our data. The cross sections is given by Eq. (3) where τ is the time constant of the exponential, j is the current density and q is the charge on the electron.

$$\sigma = \frac{q}{\tau\, j} \quad (3)$$

The magnitude of the exponentials gives us the effective density of the traps. The charge centroid correction must be used to obtain the actual density.

If we substitute the expression for the Al_2O_3 capacity into Eq. (1), we obtain for the flat band voltage shift where ε_o is the dielectric constant of Al_2O_3.

$$V_{FB} = \frac{Qt\ \bar{x}}{\varepsilon_o} \quad (4)$$

This relationship is independent of Do and thus we see that V_{FB} should not depend on Do if Qt and $\bar{x}$ are independent of Do we assume that this is the case if the implanted Al does not reach the Al_2O_3-Si interface.

Observations of breakdown phenomena were made in several ways.

The time to breakdown was recorded by photographing the oscilloscope trace of the current vs. time waveform or by recording the output of the Keithlyey 415 Electrometer on the HP 7044A X-Y recorder.

Inspection of breakdown damage was using Microscope, and was recorded on Polaroid Film. But details of the results of dielectric breakdown studies were described in this paper.

3. EXPERIMENTAL RESULTS

One method of studying dielectric breakdown is to apply a constant high voltage to the sample and observe the I-t behavior. Fig. 2. shows the behavior of the current for an applied bias of + 22V on a 450Å film of Al_2O_3 with Al metalliza-

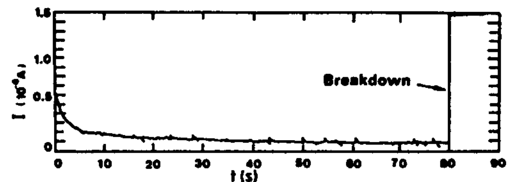

Fig. 2. Current (I) vs. time (t) for +22 V bias on Al-(450Å)Al_2O_3-n-Si.

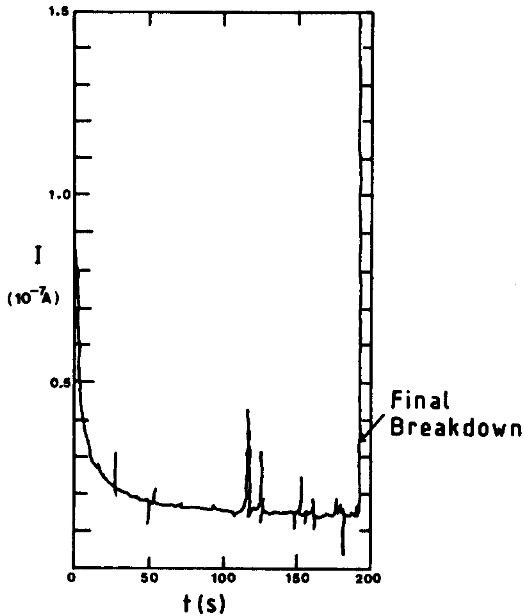

Fig. 3. Typical current decay for Au-(510Å)Al_2O_3-n-Si for +27.5 V bias.

tion and n-Si substrate. After the application of bias the current first rises rapidly to a peak (which is much greater than that shown in Fig. 2. because of the X-Y recorder's relatively slow response time) and then decays monotonically. At t= 80s, we see a sharp rise in the current, corresponding to electrical breakdown of the Al_2O_3.

This is a typical result obtained with Al electrodes. In some samples, we observed a small fluctuation in current prior to breakdown, similar to what Tsujide et al. reported.[12]

We were not able to see this fluctuation in all cases. Fig. 3. shows a typical I-t curve obtained with a gold electrode. The spikes in the curve correspond to self-quenching breakdowns (SQBD). Note that the SQBD's tend to occur with greater frequency as t increases.

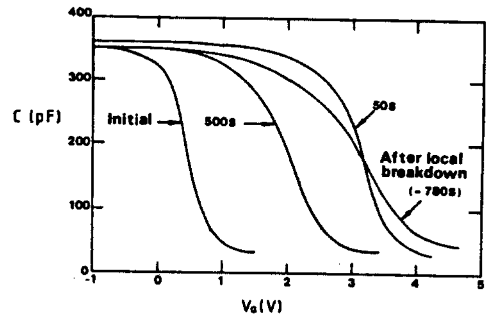

Fig. 4. Typical C-V curves before and after breakdown; -20 V bias on Al-(450Å)Al_2O_3-p-Si.

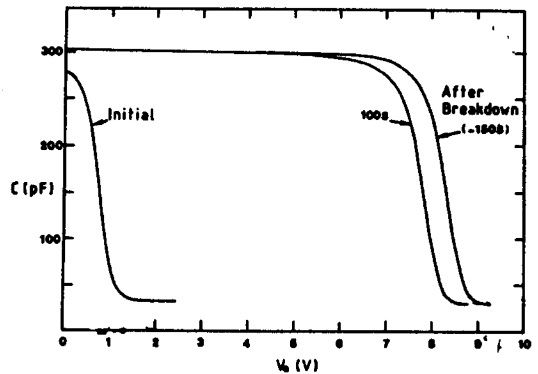

Fig. 5. Typical pre- and post-breakdown C-V curves for 18 V bias on Al-(450Å)Al_2O_3-p-Si under incandesent illumination.

Although we have found it easy to produce SQBD's in samples with Au electrodes, we have never observed them in samples with Al electrodes.

The final breakdown is not necessrily a shorting breakdown in all cases, but might be described as the switching from a low-conductivity to a high conductivity state.

This can be seen in Fig. 4, which shows C-V curves taken before and after the breakdown event, for negative bias applied to a p-Si sub-

strate, with Al electrode. Note the initial increase in ΔV_{FB} up to 25-50s, followed by a decrease, shown by the curves moving to the left. This is a typical result obtained with negative bias. Note that there is a stretchout of the C-V curve as well as a shift after breakdown. We have observed both positive and negative shifts with negative bias.

Fig. 5. shows the C-V curves before and after breakdown for positive bias on p-Si samples. Incandescent illumination was used to maintain an inversion layer. Fig. 6. shows the pre- and post-breakdown curves for an n-Si sample positively biased with Al electrode. The hump of the post-breakdown curve is due to the capacitance meter being "fooled" by the large leakage current. Nevertheless, we see that the post-breakdown curve is shifted back almost to the initial C-V curve. Fig. 5 and Fig. 6 show the typical results for negative bias applied to a Au-plated oxide. Here again we observe a negative flat band shift immediately following breakdown. In this case there is also distortion of the C-V curve.

The determination of the breakdown strength of Al_2O_3 is not straightforward. The usual method of applying a voltage ramp to the MOS capacitor and measuring the voltage at which the sample breakdown is not adequate. Because of charging effects, the breakdown voltage measured by the ramp technique will depend on the ramp rate : the greater the ramp rate, the greater will be the breakdown voltage. An alternative method is to apply a fixed bias and measure the time to breakdown. By making a series of such measurements at different biases, we obtain curves such as are displayed in Fig. 8. As the curves do not approach a limiting field as $t \rightarrow \infty$, we shall define the breakdown field at an arbitrary time, such as $t = 10^3$s, The quoted break-

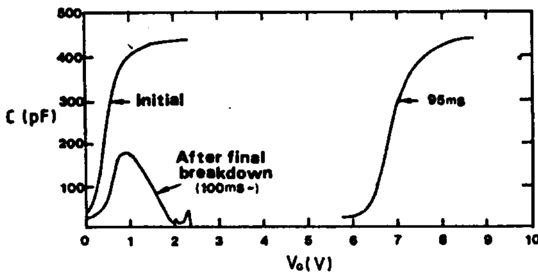

Fig. 6. Typical pre- and post-breakdown curves for +22 V bias on Al-(450 Å) Al_2O_3-n-Si.

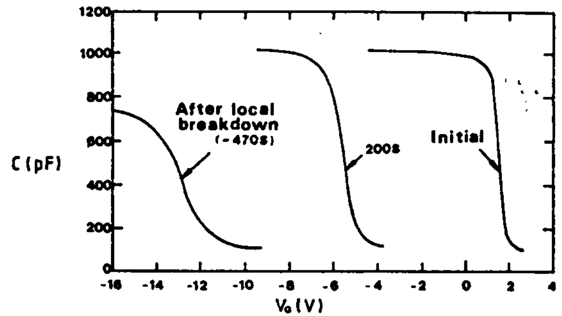

Fig. 7. Typical pre- and post-breakdown curves for −32.5 V bias on Au-(510 Å) Al_2O_3-p-Si.

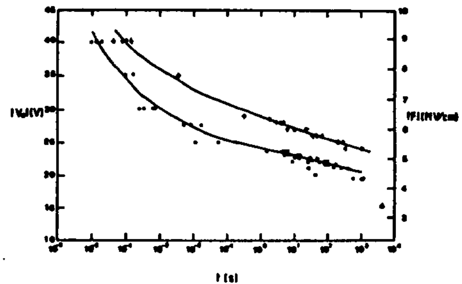

Fig. 8. Applied field, F vs. time to breakdown, t
● : positive bias on Al-(450 Å) Al_2O_3-n-Si
X : negative bias on Al-(450 Å) Al_2O_3-p-Si

down field is the average field in the oxide, not the maximum field. Note also that there is a difference of 1MV/cm in the breakdown field for negative bias and for positive bias. Observation of Fig. 8 shows that the breakdown field is about 4.5 MV/cm for positive bias and about 5 MV/cm for negative bias on-Si.

Measurements made with Au electrodes give approximately the same value of breakdown field as with Al electrode for positive bias on n-Si, but a value of 6.5MV/cm for negative bias on p-Si.

4. DISCUSSION OF EXPERIMENTAL RESULTS

The interpretation of the experimental studies of breakdown is facilitated by considering the band diagram of Fig. 9. In Fig. 9(a) we show the initial band configuration of the MOS capacitor under negative bias. If the applied field is greater than the threshold for injection, then electrons will be injected from the metal. In the recent papers, we know that, at least initially, these electrons will be trapped close to the metal. This produces the situation of Fig. 9(b). The electron trapping has caused the field at the metal interface to diminish. This, in turn, reduces electron injection from the metal.

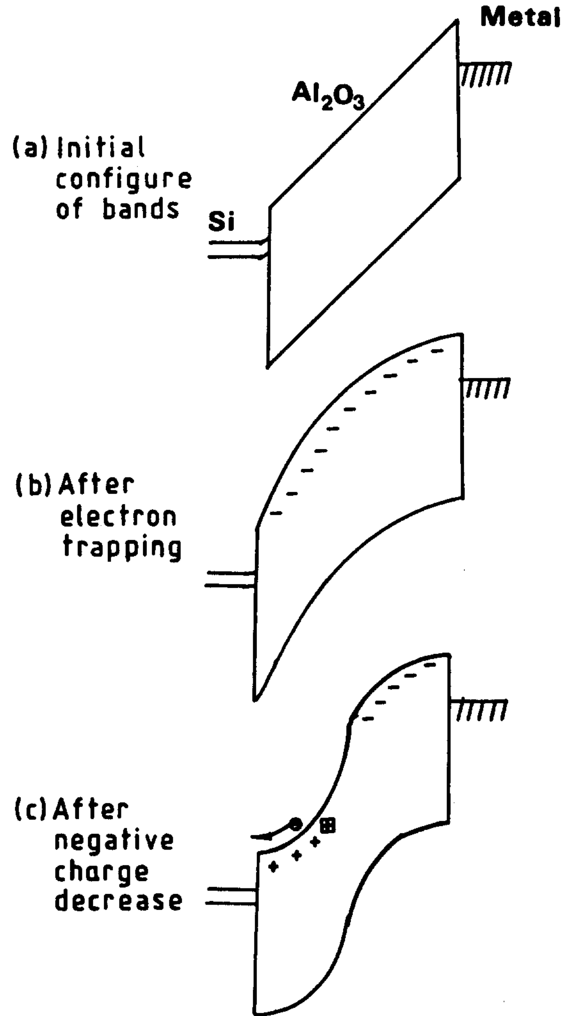

Fig. 9. Model of electronic charging and breakdown mechanism; negative bias.

Consequently, the current diminishes, as indicated in Fig. 2. From Fig. 9 (b) we can see that, which the field at the metal interface decreases, the field at the semiconductor interface must increase to maintain the same average field. If the Si interface field is high enough, we may have (1) hole injection and trapping and/or (2) electron emission from donor centers in the oxide. It is either or both of these processes which cause the phenomenon of flat band voltage reduction under negative bias. Then we have the band bending shown in Fig. 9 (c). Note that since the Si interface field has now decreased, the field in the bulk of the oxide has increased. Hole injection and trapping will act to reduce the interface field : this is a self-quenching process. Therefore, it cannot itself lead to breakdown. On the other hand, electron emission from donor centers

in the bulk, which results in additional increase in the electric fied. This process is thus unstable in the sense that once the critical field for electron emission is self-enhancing (positive feedback).

The current due to the enhanced electron emission from traps may not be large enough to produce a noticeable increase in the external current until the field is very large. Then the current increase can be extremely rapid and can only be observed with a fast oscilloscope.

The model for breakdown with positive bias is similar, except that the interfaces in the above discussion are changed.

The absence of the flat band boltage decrease phenomenon can be easily explained. With positive bias, the electron injection and trapping occurs near the silicon interface, increasing the field at the metal interface. The electron emission from traps will therefore take place near the metal interface. Since the flat band voltage is proportional to the centroid of the trapped charge measured with respect to the metal interface, any positive charge near the metal can be masked by negative charge near the silicon, and there may not be any measurable flat band voltage decrease. Singh and Anand[13] have explained the difference in breakdown strength for negative and positive bias as due to the presence of positivily charged surface states at the silicon interface.

The model which employs electron emission from traps rather than hole injection and trapping is also in good agreement with the results of a recent paper.[14]

Impact ionization is probably not as significant in Al_2O_3 as it is in SiO_2.[15, 16] The mean free path is about 10 Å, as compared to about 34 Å for SiO_2. This implies that, if impact ionization were the dominant breakdown mechanism, we would observe a much higher breakdown strength in Al_2O_3 than in SiO_2.

This is not the case. Also, in SiO_2 a current multiplication effect is observed prior to breakdown. This is a steady increase in the current which occurs over a period of seconds to minutes. No such effect was seen in Al_2O_3. Finally, if impact ionization were important, the breakdown strength should decrease as one goes to low temperatures because the mean free path increases at lower temperature. However, an increase, rather than a decrease, in the breakdown strength of Al_2O_3 is observed at low temperatures.[12] These results make impact ionization seem unlikely to be of importance in the breakdown of Al_2O_3.

5. CONCLUSIONS

Aluminum oxide (Al_2O_3) offers some unique advantages over the conventional silicon dioxide (SiO_2) gate insulation; possibility of obtaining low threshold-voltage MOSFETs, and possibility of use as in nonvolatile memory devices. We have undertaken a study of the high-field properties of Al_2O_3 on Si deposited by GAIVB Techique.

Our test structures were metal-aluminum oxide-silicon (MAS) capacitors with both aluminum and gold field plates. The major prob-

lem with Al_2O_3, when used as a gate insulator, is its flat band voltage instability under moderate bias levels ($>$ 1MV/cm)

This is caused by trapping of electrons in the oxide.

We have explored the mechanism of charge injection and trapping from both a theoretical and an experimental viewpoint.

In this paper, the dielectric breakdown of Al_2O_3 was also studied. It was found that, because of the continuous buildup of space charge, a consistent determination of breakdown strength could not be made using a ramp voltage waveform. Instead, a study was done of the time to breakdown for a given fixed bias. The average fields required to produce breakdown in 10^3 sec were approximately 4.5MV/cm for positive bias on either Al or Au field plates, 5.0 MV/cm for negative bias on Al, and 6.5 MV/cm for negative bias on Au. These fields correspond to the threshold for the onset of the high field conduction mechanism. Thus, we have additional support for the model in which instability is brought about by field emission of electrons from initially neutral centers, thus producing positive space charge near the positive interface. Hole injection through this interface, followed by trapping, would be a self-limiting process, whereas the buildup of space charge caused by field emission would tend to cause further field emission.

We investigated the physical damage produced by breakdown. The use of thin (200Å and 1000Å) Al and Au field plates made this possible. With Au field plates, we observed self-quenched breakdowns(SQBDs) before the final shorting breakdown. With Al field plates, we never observed SQBDs. We surmised that this might be due to the difference in the bonding properties of Au and Al to Al_2O_3.

Another phonomenon that we observed was an apparent edge effect, that is, the majority of breakdown sites occuring in samples with Al field plates were located at or near the edge of the field plate. This effect was particularly noticeable in samples with square field plates, where the breakdown sites were frequently to be found at the corners of the field plates, as might be expected from the field enhancement there.

REFERENCES

1) N. M. Johnson and M. A. Lampert; *J. Appl. Phys.*, **46**, 1216(1975)
2) S. M. Sze; *Physics of Semiconductor Devices*, John Wiley and Sons Inc. (1985)
3) E. H. Nicollian and C. N. Berglund; *J. Appl. Phys.*, **41**, 3052(1970)
4) D. J. Di Maria, J. M. Aitken and D. R. Young; *J. Appl. Phys.*, **47**, 2740(1976)
5) W. S. Johnson and J. H. Gibbons; *Projected Range Statistics Semiconductors and Related Materials*, 2nd Edition, John Wiley and Sons. Inc. (1975)
6) R. H. Walden; *J. Appl. Phys.*, **43**, 3(1972)
7) L. F, Mondolfo; *Aluminum Alloy-Structure & Properties, Buttworth CO. LTD.*
8) *Kiyoto. Linda and Tohru Tsujide; Jap. J. Appl. Phys.*, 11(6), 840(1972)
9) D. A. Mehta, S. R. Batler and F. J. Feigl; *J. Electrochem. Soc.*, **120**, 1707(1973)

10) M. Y. Sung et al; *15th Int. Conf. on Metallurgical Coatings and 1988 Vacuum Metallurgy Conf.* on Special Meeting, April 11-15, 1988 San Diego, CA.

11) M. Y. Sung et al; *35th National Symposium American Vacuum Society,* Oct., 3-7, 1988, Atlanta, GA.

12) T. Tsujide, S. Nakanuma and Y. Ikushima; *J. Electrochem. Soc.,* **117**(5), 703(1970)

13) S. Singh and K. V. Anand,; *Thin Sol. Films,* **37**, 453(1976)

14) J. J. O'Dwyer; *The Theory of Electrical Conduction and Breakdown in Solid Dielectrics,* Clarendon Press, Oxford, (1973)

15) F. B. Molean and P. S, Windour; *IEEE Trans. Nucl. Sci.,* **NS-21**, 47(1974)

16) J. A. Aboaf; *J. Electrochem. Soc.,* **114**(9), 948(1967)

17) M. Y. Sung and B. Cowell; *J. of Vacuum Science and Technology,* **A-7**, (3), 792(1989)

18) N. Klein; *Electrical Breakdown in Solids,* Academic Press, New York, (1969)

19) C. N. Berglund and R. J. Powell; *J. Appl. Phys.,* **42**, 573(1971)

(1990년 4월 12일 접수)